

# Modeling & Simulation of Air-to-ground Propagation Channel

Hamidreza Keshavarzadeh

Department of Electrical and Computer Engineering,  
Majlesi Branch, Islamic Azad University  
Isfahan, Iran

Ali Hashemi Talkhonchek

Department of Electrical and Computer Engineering,  
Majlesi Branch, Islamic Azad University  
Irafahan, iran

Mohsen Maesoumi

Department of Electrical and Computer Engineering,  
Jahrom Branch, Islamic Azad University  
Jahrom, Iran

Masood Mahzoon

Department of Electrical and Computer Engineering,  
Science and Research of Fars Branch, Islamic Azad  
University, shiraz, iran

**Abstract**—In the present article, the modeling and simulation of air-to-ground propagation in small-scale fading are presented based on a statistical model. In this study, some parameters such as maximum delay spread, channel delay characteristics, maximum Doppler frequency are obtained. In addition, the small-scale fading in air-to-ground channel is simulated and these parameters are evaluated. In the small-scale fading, signal changes in very short distances (usually half the wavelength) and random changes in sent signals (phase, amplitude, and delay) caused by the signal multipath due to receiving signals by receiver. Besides, the fading depth phenomenon and the effective factors in large-scale fading for this type of communication channel are investigated and the mean path loss model, the mean path changes, and the air-to-ground link budget whose results are useful for a better use of air-to-ground channel as well as point-to-point communications are modeled and presented.

**Keywords**—Component; small & large scale fading, air-to-ground channel, multipath, shadowing.

## I. INTRODUCTION (Heading 1)

The wireless channel for mobile communications can be one of the most severe impediments to reliable communication. This is particularly true for terrestrial channels, where (obstacles) in the environment can cause block of the line-of-sight (LOS) signal and multipath components (MPCs) that can be spread in both delay and spatial angle. The spread in delay causes distortion, which is more acute as signal bandwidth increases. In addition, mobility causes channel time variation and Doppler shifts [1]. All of these channel characteristics must be known -at least in a statistical sense- in order to develop a reliable communication system with appropriate countermeasures to the distortion and fading channel variations. Hence, many years of effort have gone into the quantitative characterization of wireless channels. For the air to ground case, obstructions are primarily of two types: ground-based obstructions such as buildings and terrain, and airframe obstructions. Both these types of objects can also cause reflections, scattering, and diffraction, yielding a multipath channel, with time variation caused by mobility.[2]

The propagation environment comprises multiple different physical effects, which affect electromagnetic waves and have a direct impact on each kind of wireless communication. In order to determine the appropriate modulation for a communication scenario, knowledge of the propagation environment is required. Exact channel characterization, meaning the deterministic way using Maxwell's equations is usually infeasible due to missing information of the propagation environment and most of all due to complexity. On this basis, the empirical way of channel sounding is normally the preferred method. Channel sounders excite the channel in order to estimate the number of multipath components (MPCs) with their associated amplitudes, phases and delays. Different sounding techniques are overviewed in[ 3]

Air-to-ground communication in the V/UHF band is widely used in civil and military avionics. The propagation channel is characterized by delay-spread, multipath fading and Doppler frequency shifts. These properties are determined by the environment and relative speed of the aircraft. Changes in the environment affect the reflection, diffraction and scattering of the signal and thus affect the channel response results in time-variant property of the channel.

The ground as well as all scattering bodies in the vicinity of the antennas is illuminated, generating multipath. Each of these reflected or scattered non-line of sight (NLOS) signals arrive at the receiver at different delays, thus creating delay-spread. The time delays are time-variant random process due to the dynamic nature of the propagation channel. Each NLOS signal also suffers from phase change caused by reflection, diffraction and scattering, which are also time-variant. The line of sight path (LOS) suffers from attenuation and delay but experiences no phase distortion. Multiple signals with independent delay, amplitude change and phase shifts results in multipath Rayleigh fading. The phase distortion is modeled as a uniform random process [4].

The delays are assumed to follow Gaussian distribution. The amplitude attenuation of each of the NLOS signals will not be the same, as the distances traveled by each of the reflected/scattered signals are not the same [5]. The phase distortion is modeled as a uniform random process. A direct path with no phase shift is also incorporated in the channel model to represent the LOS signal path. Due to the relative motion of the aircraft, the channel also suffers from Doppler frequency shifts. Large Doppler shifts can cause BER flooring [5] and therefore is an important parameter of the channel. The frequency shift is assumed to be time varying. It is modeled by a Gaussian random process. Fading and Doppler shifts can cause large number of consecutive bits to be corrupted, resulting in burst errors. The probability of burst error occurrence of the channel is computed and found to be considerably high. The burst errors degrade the BER performance of the system. To solve this problem, data interleaving and error correcting codes are used [6].

To design a wireless communication system, it is necessary to assess the performance and reliability in a particular application scenario. Due to the effects of terrain, atmosphere and other factors, the propagation of radio waves in the aeronautical channel will have a complex reflection, scattering and diffraction, resulting severe multipath fading. In broadband wireless air-to-ground communications, both the velocity and acceleration of an aircraft are very large. There exists a variety of studies that characterize the air-to-ground wireless link. The effect of indirect paths scattered from the surface of the earth is focused in [7], where a class of aeronautical wide-band channel models was proposed, featuring parking and taxi environments, takeoff and landing situations, and en-route scenarios for ground-air and air-air links, and both the typical and worst case parameter sets are suggested based on published measurements results and empirical data. When the aircraft is far away from the ground station and the antenna of the ground station is very small. Under such circumstances, the reflected signals of the ground objects will lead to a serious multi-path propagation, the antenna elevation angle will increase with decreasing communication distance of the ground station to aircraft, and the reflection signal caused by ground objects will be reduced. In addition, the multipath propagation delay caused by reflection is relatively large, which can reach hundreds of microseconds. The power of multipath signal components shows a decreasing trend with the increase of the relatively time delay values. [8]

Regarding one sender in the airplane and several receivers with specified locations on the earth, we want the propagation channel small-scale fading and large-scale fading to stand between the moving sender and the fixed receivers of the model. In the present article, efforts are made to determine parameters such as path loss, maximum delay spread, channel delay characteristics, maximum Doppler frequency, and other effective channel parameters. In addition, the small-scale fading in air-to-ground channel includes all parameters related to this type of modeling fading, and the obtained results can be used to improve the use of this type of channel and to better control the air traffic and a secure communication.

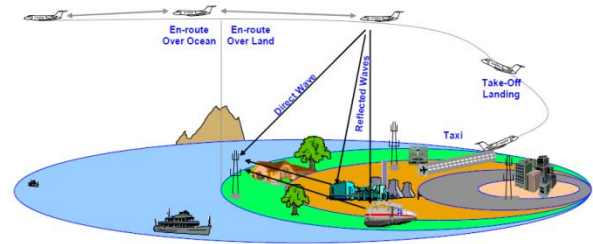


Fig. 1. Aeronautical channel

## II. AIR-TO-GROUND LINK POWER BUDGET

In the distance between sending and receiving antennae, radio waves undergo not only free space loss but also other excess losses caused by various phenomena in the air. The free space loss and the losses caused by the abovementioned factors are totally referred to as the main transfer loss. While the free space loss is only a function of the frequency and the distance between the sender and the receiver, the main transfer loss is also a function of atmosphere conditions and the structure of the transfer environment.

By investigating the airplane movement, we obtained the relatively exact losses from the airplane to the ground antenna to which they are imposed, and we present them as follows.

The effective send power includes the effects of radio parts as well as the transfer in sending direction. This parameter is shown as ERP and is usually stated by dBm or dBw. The effective send power is in fact the product of the output sender power after imposing the losses caused by the transfer and connection line in antenna gain in a desired direction. When the antenna gain is compared to an isotropic antenna, it is indicated as EPRP parameter:

$$ERP = P_{tr} GT / LT \quad (1)$$

where  $P_{tr}$ ,  $GT$ , and  $LT$  are the sender's power in its output (Watt), the sender's antenna gain (airplane transponder), and the losses caused by the cables and connections between the antenna and the transponder, respectively. If the power base is dBm, its logarithm form will be as follows:

$$ERP = P_{tr} + GT - LT \quad (2)$$

in which ERP and  $P_{tr}$  are according to dBm while  $GT$  and  $LT$  are according to dB

### A. Free Space Loss

Free space loss includes the path loss and the losses caused by the atmosphere, and since  $\lambda = 27.52$  cm ( $f = 1090$  MHz), our atmosphere loss with regard to our wavelength and the distance between the sender and the receiver  $d$  is shown in table (1) compared to the distance according to Nautical Mile (1.85 km).

	Distance of airborne equipment from ground station			
	0.5 N.M	100 N.M	200 N.M	250 N.M
Attenuation due to atmosphere	0.0 dB	0.9 dB	1.4 dB	1.6 dB

TABLE I. WEAKENING BY THE ATMOSPHERE FOR AIR LOS LINKS IN 1 GHZ FREQUENCY[ 9]

$$L_{\text{free space}} = \frac{1}{L_{\text{at}}} \frac{1}{R^2} \frac{\lambda^2}{(4\pi)^2} \quad (3)$$

And if R is based on Nautical Mile, the path loss and free space loss become logarithmically as follows:

$$L_{\text{path loss (dB)}} = 20\log(R) + 98.54 \quad (4)$$

$$L_{\text{free space (dB)}} = L_{\text{at}} + 20\log(R) + 98.54 \quad (5)$$

The receiving power to the ground station is:

$$P_{\text{ant}} = \text{ERP} \frac{1}{L_{\text{at}}} \frac{1}{R^2} \frac{\lambda^2}{(4\pi)^2} \quad (6)$$

λ on R is according to Watt while ERP and P<sub>ant</sub> are according to Nautical meter (NM). When the distance is according to Nautical Mile, and ERP and P<sub>ant</sub> are according to dB, its logarithmic form is follows:

$$P_{\text{ant}} = \text{ERP} - L_{\text{at}} - 20\log(R) - 98.54 \quad (7)$$

And finally, the receiving power in receiver's input is:

$$P_{\text{rec}} = P_{\text{ant}} \text{GA} / \text{LI} \quad (8)$$

in which GA and LI are the antenna gain and the fader loss, respectively.

(Air_Ground)		
200 NMI	100 NMI	
57	57	(dBm) transmitter power aircraft
-3	-3	(dB) (L <sub>7</sub> ) Cable Loss
2	2	(dBi) (G <sub>7</sub> ) gain of the transmitter antenna
-145.96	-139.44	(dB) Free space loss
4	4	(dBi) (G <sub>r</sub> ) gain of the receiver antenna
-3	-3	(dB) (L <sub>f</sub> ) Feeder Loss
-88.96	-82.44	(dBm) receiver power

TABLE II. LINK BUDGET PARAMETERS

The effective factors in air-to-ground link are shown in a block in figure (1). According to the atmosphere loss values shown in table (1), we show the free space loss diagram based on dB and the space based on Nautical Mile (NM) in figure (2). Besides, we can state and simulate the receiver antenna noise through equation (9). The simulation results are shown in figure (3).

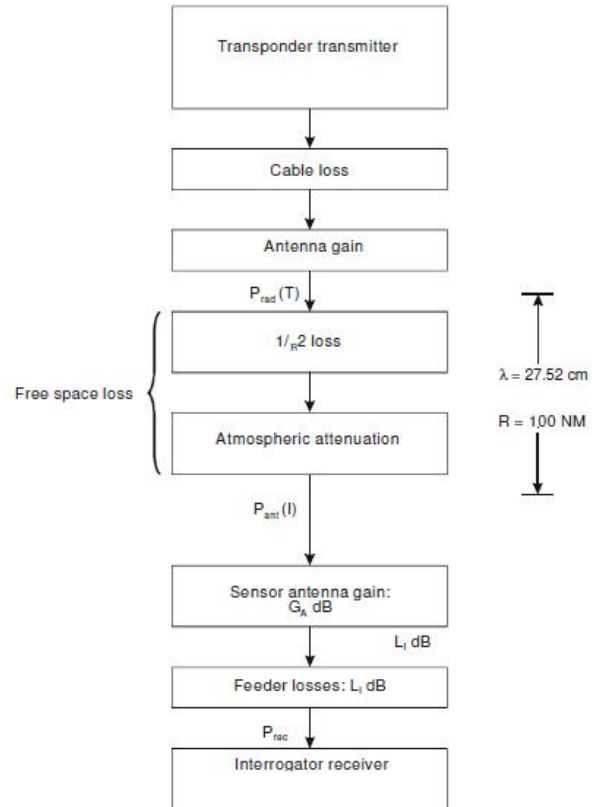


Fig. 2. Air-to-ground link diagram block

$$N_0 = k \left[ T_0 (F - 1) + \left( \frac{T_a}{L_a} + T_0 \left( 1 - \frac{1}{L_a} \right) \right) \right] * B_n \quad (9)$$

in which K is the Boltzmann constant and equals 1.38\*10<sup>-23</sup>. B<sub>n</sub>, F, and T<sub>0</sub> are the receiver's effective band width, the receiver's noise value, and the noise equivalent temperature, respectively. The antenna loss L<sub>a</sub> in the limit will be assumed 0/1 to 0/3 dB and the equivalent antenna temperature T<sub>a</sub> will be assumed 75 to 300 degrees of Kelvin in the limit.

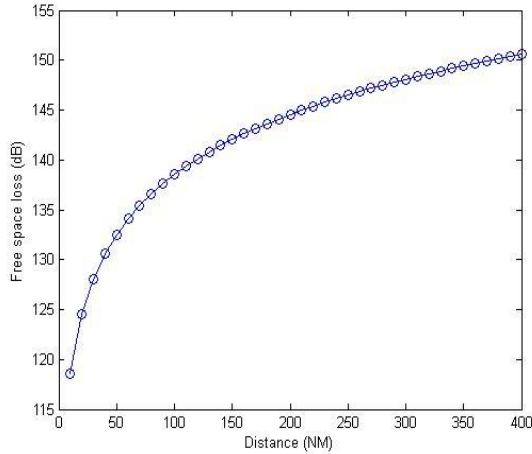


Fig. 3. Free path loss diagram based on the space

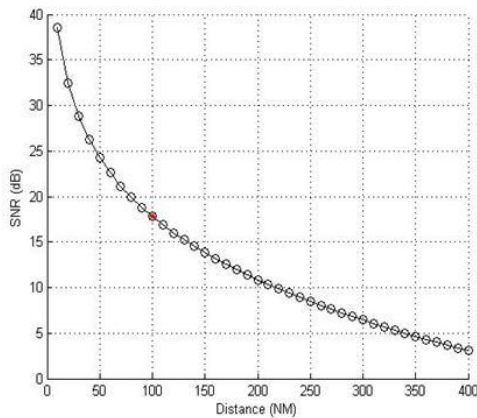


Fig. 4. Receiver noise simulation diagram

If the receiver antennae existing in the ground station locate in an area with hills, mountains and obstacles, the received power will be as follows [10]:

$$PR = \frac{P_T G_T G_R}{L_T L_R L_P} \tag{10}$$

where PR and PT are the receiver’s and the sender’s power, GT and GR are the receiver’s and the sender’s gain, LT and LR are the losses existed in the sender and the receiver (cable and fader loss), and LP is the channel propagation loss which is usually made of three components: LP= L0LSLL in which L0, LS, and LL are the average path loss (free space loss), the loss caused by obstacles (shadowing), and the loss caused by multipath, respectively. We define the fading depth

as  $F = LS LL$ .

### III. FADING DEPTH

Fading depth is defined as the total excessive propagation losses due to multipath and shadowing in comparison with the ideal free space model. The accurate estimation of fading depth is of great importance for designing communication links. This estimation is necessary for budget analysis designing link and simulation of communication systems disconnection probability.

### A. Multipath

Figure (4) shows a two-path model for air-to-ground channel and our ground environment includes an area with lots of hills, mountains, etc.

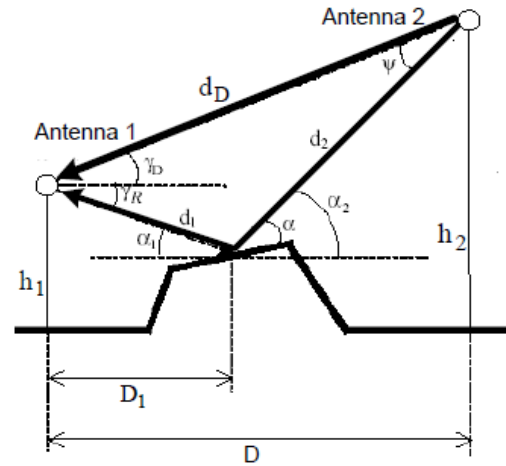


Fig. 5. A two-path model for air-to-ground propagation[10]

The total received energy in the receiver is:

$$E_{total} = |E_D + E_R e^{j\Delta\phi}| \tag{11}$$

in which ED and ER are the energy resulted from the direct and reflective paths, respectively. Δφ is the phase difference and the minimum received signal is:

$$E_{min} = E_D - E_R \tag{12}$$

The worst fading depth state occurs when  $=\pi\Delta\phi$ .

$$F = \left(\frac{E_D}{E_{min}}\right)^2 = \left(1 - \frac{E_R}{E_D}\right)^{-2} \tag{13}$$

The fading depth can be stated as follows:

$$F = \left(1 - \Gamma \frac{d_D}{d_1 d_2} + G_1(\gamma)G_2(\psi)\right)^{-2} \tag{14}$$

in which Γ is the reflection coefficient obtained from classic equations:

$$\Gamma V = \frac{-\epsilon_r \sin(\alpha) + \sqrt{\epsilon_r - \cos^2(\alpha)}}{\epsilon_r \sin(\alpha) + \sqrt{\epsilon_r - \cos^2(\alpha)}} \tag{15}$$

$$\Gamma H = \frac{-\sin(\alpha) + \sqrt{\epsilon_r - \cos^2(\alpha)}}{\sin(\alpha) + \sqrt{\epsilon_r - \cos^2(\alpha)}}$$

where V and h show horizontal and vertical polarization, and  $\epsilon_r$ ,  $\alpha$ ,  $G(\gamma)$  and  $G(\psi)$  are ground electric permittivity coefficient, signal exit angle after the reflection, normalized pattern in reflection direction for ground antenna and normalized pattern for aerial antenna, respectively. We assume the following:

$$D \gg h_1, h_2 ; h_2 \gg h_1 ; G(\gamma)=1 \text{ and } G(\psi).$$

$$\Gamma_V \approx 1 - 2 \alpha \sqrt{\epsilon_r} \Gamma_H \approx 1 - 2 \alpha / \sqrt{\epsilon_r} \quad (16)$$

The fading depth resulted from multipath is obtained by:

$$FV \approx \frac{1}{\gamma^2 \epsilon_r} \quad FH \approx \frac{\epsilon_r}{\gamma^2} \quad (17)$$

Figure (5) shows the results of fading depth caused by multipath for horizontal and vertical polarization in 1 GHz frequency.

**B. Shadowing**

Shadowing is the slow changes observed around the average path loss that is due to the existence of obstacles. In this regard, we divide the channel path into three groups: direct path (LOS), direct pass somewhat weakened by trees' leaves and branches (OLOS), and the path blocked by one or more buildings (NLOS).

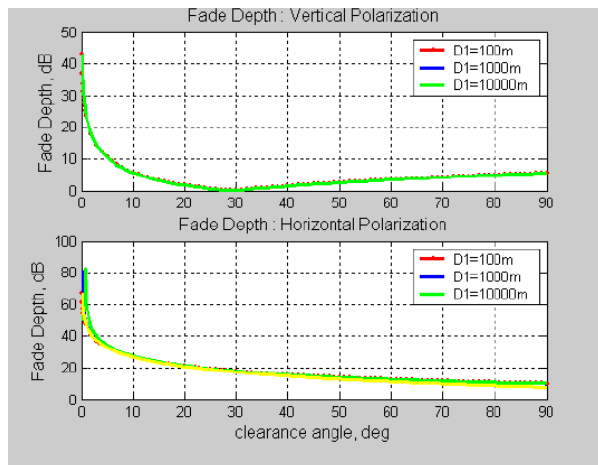


Fig. 6. Simulation results of fading depth caused by multipath

Frequency	LoS (Mean path loss variation)							
	100m		200m		500m		1000m	
	$\rho$	$\gamma$	$\rho$	$\gamma$	$\rho$	$\gamma$	$\rho$	$\gamma$
200MHz	0.0143	0.9941	0.0153	0.9131	0.0214	0.7308	0.0418	0.4746
1000MHz	0.0154	0.9751	0.0218	0.8135	0.0186	0.7512	0.0307	0.5455
2000MHz	0.0187	0.9268	0.0338	0.6935	0.0375	0.5367	0.0536	0.3426
2500MHz	0.0148	0.9843	0.0272	0.7475	0.0306	0.5901	0.0389	0.4256
5000MHz	0.0086	1.1222	0.0140	0.8926	0.0181	0.7236	0.0184	0.6186
Frequency	LoS		OLOs (Shadowing)		NLoS (Shadowing)			
	$\rho$	$\gamma$	$\rho$	$\gamma$	$\rho$	$\gamma$	$\rho$	$\gamma$
200MHz	0.0513	0.3656	0.3334	0.3967	0.7489	0.4638		
1000MHz	0.0353	0.4730	0.5568	0.3598	1.5036	0.3200		
2000MHz	0.0499	0.2975	0.6877	0.3619	2.1139	0.2508		
2500MHz	0.0398	0.3179	0.7224	0.3643	2.3197	0.2361		
5000MHz	0.0160	0.5574	0.8937	0.3713	2.7940	0.2259		

TABLE III. PARAMETERS FOR SHADOWING MODELS[11]

The formula below has been provided for shadowing:

$$\sigma_x[\text{dB}] = \rho(90 - \theta)^\gamma \quad (18)$$

and its values can be extracted from table (3) [11]. The total fading depth is stated as follows:

$$F \approx (1 - \Gamma)^{-2} + \sigma^2 \quad (19)$$

$$FV \approx \frac{1}{\gamma^2 \epsilon_r} + \sigma_x^2 \quad FH \approx \frac{\epsilon_r}{\gamma^2} + \sigma_x^2 \quad (20)$$

**IV. ANALYZING A MULTIPATH CHANNEL IN AN AIR-TO-GROUND CHANNEL**

The Impulse response of a propagation channel with amplitude  $\alpha$  and delay  $\tau$  for various times can be shown as [12]:

$$h(\tau, t) = \sum_{n=0}^{N(t)} \alpha_n(t) e^{-j\phi_n(t)} \delta(\tau - \tau_n(t)) \quad (21)$$

Where;

$N(t)$  – the number of the multipath signal components present in the channel (at time t)

$\tau_n(t)$  – the delay of the nth multipath signal component

$\alpha_n(t)$  – the amplitude of the nth signal multipath component

$\phi_n(t)$  – the phase shift associated with the nth multipath component.

The phase element,  $\phi_n(t)$  contains the contributions from multipath delay,  $\phi_{\tau_n}$  and

doppler shift,  $\phi_{d_n}$  of each multipath component and is denoted as:

$$\phi_n(t) = \phi_{\tau_n}(t) + \phi_{d_n}(t) \quad (22)$$

**A. Doppler Shift**

The doppler shift of the nth multipath component,  $f_{d_n}(t)$  due to the receiver's motion is

given by:

$$f_{d_n}(t) = \frac{vc \cos \theta(t)}{\lambda} \quad (23)$$

The receiver's motion gives rise to phase shifts of each reflected multipath element. As a

result the signal amplitude varies randomly. The angle of arrival is assumed to be

uniformly distributed between  $[-\pi, \pi]$ . The phase shift associated with the Doppler

frequency is:

$$\Phi_{d_n} = \int 2\pi f_{d_n}(t) dt \quad (24)$$

**B. Multipath delay**

Multipath delay,  $\tau_n(t)$  is the measure of the time that the  $n$ th multipath signal takes to arrive at the receiver. Delay for individual multipath component at the receiver is calculated by using their corresponding path length,  $r_n(t)$  and the speed of light,  $c$ .

$$\tau_n(t) = \frac{r_n(t)}{c} \quad (25)$$

The phase shift related to the delay is

$$\phi_{d_n} = e^{-j\pi f_c \tau_n(t)} \quad (26)$$

For constant times, the receive signal in  $y(t)$  output equals the convolution of sent signal  $x(t)$  in the stroke response:

$$y(t) = \sum_{n=0}^{N-1} \alpha_n e^{-j\phi_n} \delta(\tau - \tau_n(t)) * X(t) \quad (27)$$

$$y(t) = \sum_{n=0}^{N-1} \alpha_n e^{-j\phi_n} x(\tau - \tau_n) \quad (28)$$

where the sender's signal  $x(t)$  is made of a pulse  $p(t)$  with unit amplitude and TP width.

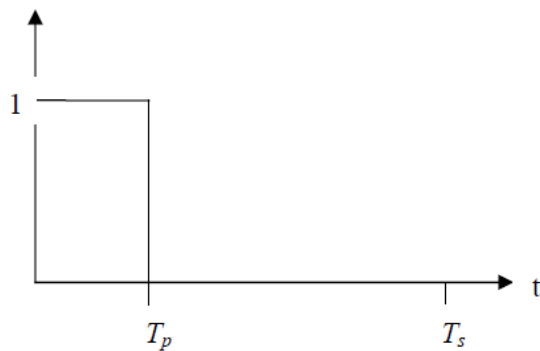


Fig. 7. A signal pulse form with the width TP

$$X(t) = P(t) = \begin{cases} 1 & 0 \leq t \leq T_p \\ 0 & \text{otherwise} \end{cases} \quad (29)$$

The sent pulse is shown as modulated with the carrier frequency  $f_c$ :

$$X(t) = P(t) e^{j2\pi f_c t} \quad (30)$$

And the received signal becomes as follows:

$$y(t) = \sum_{n=0}^{N-1} \alpha_n e^{-j\phi_n} P(t - \tau_n) e^{j2\pi f_c t} + w(t) \quad (31)$$

in which  $W(t)$  is the white noise.

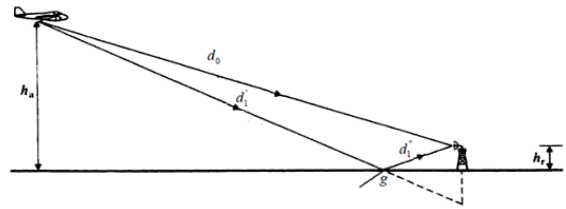


Fig. 8. The direct path LOS and the ground reflective path

According to figure (8), the received signal power includes the LOS signal power and the ground reflection power.[ 11]

$$E_{\text{received}} = E_{\text{LOS}} + E_{\text{ground reflected}} \quad (32)$$

In figure (8),  $d_0$ ,  $d_1$ ,  $d_1'$ , and  $g$  are the distance between sender and receiver, the distance to reflective point (before reflection), the distance from reflective point to the receiver, and the reflective point, respectively. Therefore, we receive the signal and divide it into two classified states:

Signal power using direct path

$$P(t) = \begin{cases} 1 & \frac{d_0}{c} \leq t \leq \frac{d_0}{c} + T_p \\ 0 & \text{otherwise} \end{cases} \quad (33)$$

According to equation (31), we define amplitude  $\alpha_0$ , delay  $\tau_0$ , and Doppler frequency  $f_{d_0}$  parameters.

$$\alpha_0 = \frac{\sqrt{30 P_t G_t}}{d_0} \quad (34)$$

$$\tau_0 = \frac{d_0}{c} \quad (35)$$

$$f_{d_0} = \frac{2\pi v \cos \theta_0}{\lambda} \quad (36)$$

Signal power as a result of ground reflection and direct path with reflection coefficient

$$P(t) = \begin{cases} 2A_p \frac{d_1' + d_1''}{c} \leq t \leq \frac{d_1' + d_1''}{c} + T_p \\ 0 & \text{otherwise} \end{cases} \quad (37)$$

According to equation (18-2), we define amplitude  $\alpha_0$ , delay  $\tau_0$ , and Doppler frequency  $f_{d_0}$  parameters.

$$\alpha_1 = \Gamma_g \frac{\sqrt{30 P_t G_t}}{d_0} \quad (38)$$

$$\tau_1 = \frac{d_1' + d_1''}{c} \quad (39)$$

$$f_{d_1} = \frac{2\pi v \cos \theta_1}{\lambda} \quad (40)$$

### C. Small scale fading channel parameters

In order to compare different multipath channels and to develop some design methods for mobile communication systems, different parameters which grossly quantify the channel are used. We can classify the parameters into 2 categories: time dispersion and frequency dispersion parameters. Channel parameters that describe time dispersive .

#### 1) Time dispersion parameters

The mean excess delay  $\bar{\tau}$  is the first moment of the power delay profile of the

pulse signal and is defined as [13]

$$\bar{\tau} = \frac{\sum \alpha_n^2 \tau_n}{\sum \alpha_n^2} = \frac{\sum p(\tau_n) \tau_n}{\sum p(\tau_n)} \quad (41)$$

$$\bar{\tau}^2 = \frac{\sum \alpha_n^2 \tau_n^2}{\sum \alpha_n^2} = \frac{\sum p(\tau_n) \tau_n^2}{\sum p(\tau_n)} \quad (42)$$

The RMS delay spread  $\delta\tau$  is the square-root of the second moment of the power

delay profile. The RMS delay spread is a measure of time dispersion in the

channel.

$$\sigma_\tau = \sqrt{(\bar{\tau}^2) - (\bar{\tau})^2} \quad (43)$$

Coherence bandwidth  $B_c$  is the statistical measure of frequencies over which the

channel can be considered "flat". It describes the point at which two

frequencies of a signal are likely to experience comparable amplitude fading. This

property is related to the rms delay spread as follows;

$$B_c \propto \frac{1}{\sigma_\tau} \quad (44)$$

- For a bandwidth over which the frequency correlation function is above 90% or 0.9, the coherence bandwidth is given as [14];

$$B_c \approx \frac{1}{50 \cdot \sigma_\tau} \quad (45)$$

If a coherence bandwidth  $B_c$  describes a bandwidth over which the frequency correlation function is above 50% or 0.5 then it is approximated

as follows;

$$B_c \approx \frac{1}{5 \cdot \sigma_\tau} \quad (46)$$

#### 2) Frequency dispersion parameters

Doppler spread,  $B_D$  shows the spectral broadening due to effect of the doppler shift,  $f_d$ . It is the effect from the movements of the receiver/reflectors in the channel. These movements cause the variation of signal's frequency during transmission through each multipath. This means signals traveling in different

multipath have different Doppler shift. The Doppler spread shows the spectral spreading caused by the time rate of change of the wireless propagation channel due to the relative motions of receiver/reflectors with respect to the base stations

$$B_D = f_m \quad (47)$$

Where  $f_m$  is the maximum Doppler shift and is denoted as;

$$f_m = \frac{v}{\lambda} \quad (48)$$

Coherence time  $T_c$  is inversely related to Doppler spread and is expressed as follows;

$$T_c \propto \frac{1}{f_m} \quad (49)$$

Coherence time is the statistical measure of the time duration over which the channel impulse response is essentially invariant, and quantifies the similarity of the channel response at different times . It describes the duration of time at which two signals at the receiver experience possible amplitude correlation.

- If this coherence time is defined at the time over which the time correlation function is over 50% or 0.5 then coherence time is denoted as:

$$T_c \approx \frac{9}{16\pi f_m} \quad (50)$$

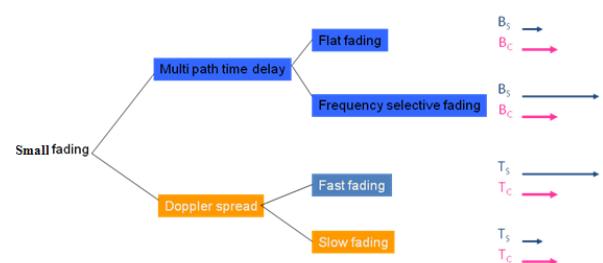


Fig. 9. small scale fading Categories

typical value	symbol	channel parameters
1090 MHz	$f_c$	carrier frequency
8 MHz	$B_w$	Band width
900 Km/h	$v$	speed aircraft
16 MHz	$F_s=2B_w$	frequency sampling
$6.25 \times 10^{-8}$	$T_s=1/F_s$	time sampling
15dB	$K_{Rice}$	Rician K Factor
833 Hz	$F_d=f_c v/c$	Maximum doppler Frequency
27.52 cm	$\lambda$	wave length

TABLE IV. VARIABLE CHANNEL PARAMETERS

According to the sampling frequency ( $2 \cdot B_s$ ) twice as wide as the band and the sampling time ( $1/F_s$ ) it can be concluded that TS value is much smaller than correlation time TC. Therefore, the fading type is slow. In addition, regarding the band width (8MHz) that is larger than correlation width, it might be concluded that the fading frequency is selective.

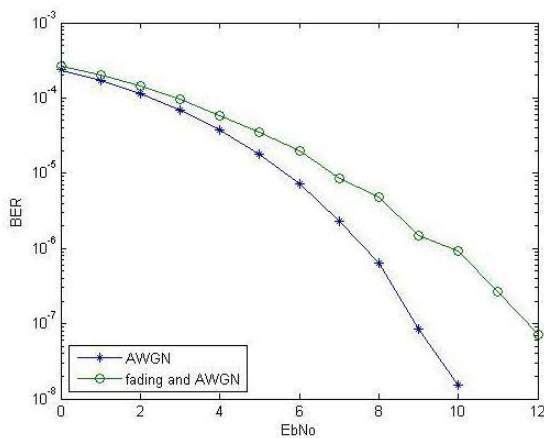


Fig. 10. BER changes diagram for Rician slow fading based on EbN0

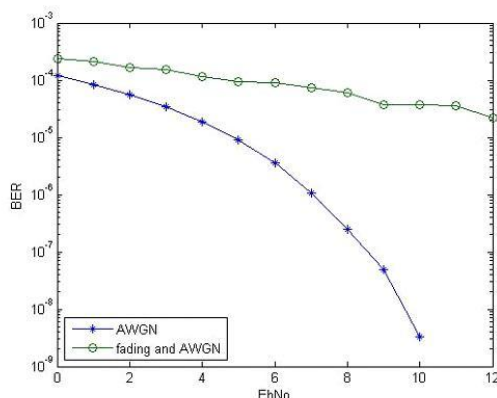


Fig. 11. BER changes diagram for Rayleigh slow fading based on EbN0

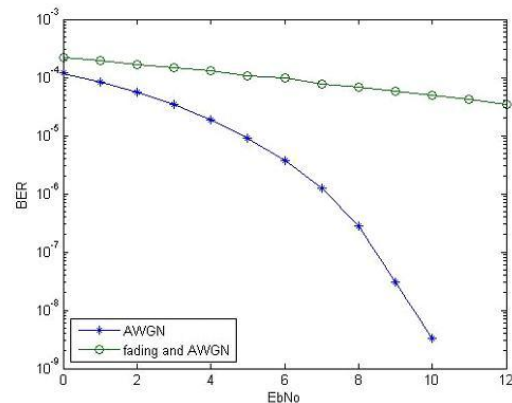


Fig. 12. BER changes diagram for Rayleigh selective frequency fading based on EbN0

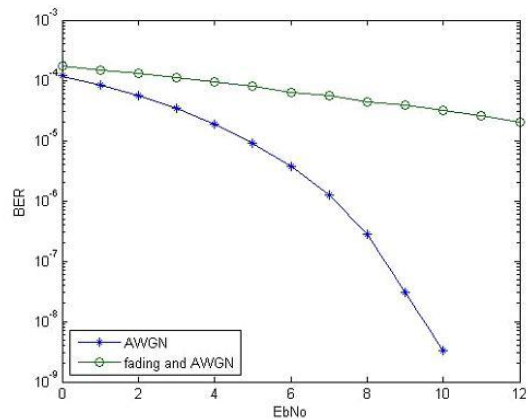


Fig. 13. BER changes diagram for Rician selective frequency fading based on EbN0

It is clear that, the performance of Rician model is better than Rayleigh model cause of existing strong direct line of sight(LOS) and in fading conditions, the selective frequency, time dispersion due to multi-path phenomenon is high and received signal making some copies of submissions signals and also according to existence of inter symbol interference(ISI) has better performance than slow fading conditions.

### V. CONCLUSIONS

The effects of some phenomena such as rain, snow, hail, cloud and fog in the air were investigated. In general, regarding rain drops and the drops existing in clouds, fogs have a diameter smaller than 0.1 millimeter and would be effective for high frequencies. All these phenomena are ignorable in 1GHz frequency.

According to table (3), the shadowing phenomenon is dependant on frequency and airplane height for LOS state, while it is dependant only on frequency for OLOS and NLOS states. Hence, it can be seen that for OLOS and NLOS states, as the frequency increases the reflection and diffraction increase, too. Due to the blockage of OLOS path by trees' leaves and branches, there exists less loss compared to NLOS. Hence, the total loss is as follows:



Total loss = path loss + atmosphere loss + fading depth + loss related to connections (cable and fader)

Moreover, some parameters of large-scale fading including path loss, average path loss, and fading depth were stated and investigated. It is clear that in Rician model, due to the existence of strong LOS, the channel performs better than it does in Rayleigh model. In air-to-ground radio link of the Singular system, in addition to the parking scenario there always exist LOS conditions and since the main mission of this system is navigation along the path, other scenarios including parking scenario are less important.

Regarding maximum Doppler frequency and the sent signal bandwidth, the channel will always have slow fading. Since in en route flying scenario the maximum delay time is much longer than the pulse width, the channel will be frequency selective and the ISI phenomenon will be applied in simulation. In taxi and parking scenarios, since the maximum delay time is equal to or longer than the pulse width, the channel will still be frequency selective, and in entering and take off scenarios, the channel will have flat fading due to maximum delay time.

## REFERENCES

- [1] J. D. Parsons, *The Mobile Radio Propagation Channel*, John Wiley & Sons, New York, NY, 2000.
- [2] David W. Matolak, Ruoyu Sun, "Air-Ground Channel Measurements & Modeling For UAS Integrated Communications," Navigation and Surveillance Conference (ICNS), 2013 .
- [3] A. Molisch, *Wireless Communications*, 2nd ed. Wiley, ch. 6, 7, 2011.
- [4] John G. Proakis , and Masoud Salehi, *Communication System Engineering*, 2nd Edition, Pearson Prentice Hall, 2006.
- [5] Bo Zheng , Qing-huaRen, Yun-jiang Liu, and Zhen-yong Chu, "Simulation of two V/UHF air-to-ground communication channel models", International conference on wireless communication, networking and mobile computing, 2007.
- [6] Mohammad Asif Zaman, Sayed Ashraf Mamun\*, Md. Gaffar, Md. Mushfiqul Alam ,Md. Imran Momtaz," Modeling VHF Air-to-Ground Multipath Propagation Channel and Analyzing Channel Characteristics and BER Performance", IEEE Region 8 SIBIRCON-2010, Irkutsk Listvyanka, Russia, July 11- 15, 2010.
- [7] Erik Haas, Aeronautical channel modeling, IEEE Transactions on vehicular technology, VOL. 51, NO. 2, MARCH 2002.
- [8] MA Jun, ZHANG Chunsheng, TANG Liang, YUAN Wei, YU Kai, ZHENG Min," Aeronautical Channel Modeling and Simulation", proceedings of the 31 sthinese control conference july 25-27, hefei, china, 2012.
- [9] Michael C. Stevens, *Secondary Surveillance Radar*, Artech House, 1988.
- [10] S. Loyka, A. Kouki, F. Gagnon, Fading Prediction on Microwave Links for Airborne Communications, Department of Electrical Engineering, Canada.
- [11] Qixing Feng, Joe McGeehan, Eustace K. Tameh, and Andrew R. Nix, Path Loss Models for Air-to- Ground Radio Channels in Urban Environments, 2006 IEEE.
- [12] T. S. Rappaport, *Wireless Communications, Principles and Practice*, Prentice Hall, New Jersey, 1996.
- [13] Nathan Blaunstein, Christos G. Christodoulou, *Radio Propagation and Adaptive Antennas for Wireless Communications Links*, John Wiley & Sons, Inc., New Jersey, 2007.
- [14] Andrea Goldsmith, *Wireless Communications*. Cambridge University Press, 2005.